17th World Conference on Earthquake Engineering, 17WCEE
Sendai, Japan - September 13th to 18th 2020

SOURCE PROPERTIES FROM THE SLIP-WEAKENING MODEL

H. Choi[(1)], A. Baltay[(2)], B-I. Yoon[(3)]

[(1)] *CTO, AIMAC Structure Co., Ltd., hchoi01@aimac.co.kr*
[(2)] *Research Geophysicist, US Geological Survey, abaltay@usgs.gov*
[(3)] *CEO, AIMAC Structure Co., Ltd., biyoon@aimac.co.kr*

Abstract

Scaling relation based on the slip-weakening model developed by Ohnaka and Yamashita is extended beyond the breakdown (or cohesive) zone and the source properties from the extended model (SWM) are compared to those from the most widely used one by Eshelby and Keylis-Borok with Brune's nondimensional corner frequency (EBM). SWM shows that the source properties greatly depend on the rupture velocity ratio to S wave velocity, say *k*, which can be determined from the spectral corner frequency and the source-controlled cutoff frequency. From the comparison, two models show different correlation characteristics between static/dynamic scaling parameters and the seismic moment M_o. For the case of stress drop, two models show contradict correlation characteristics to the size of earthquakes, but the correlation is relatively weak in each model. On the other hand, SWM gives anti-correlation between stress drop and *k* as expected by Causse and Song. The degree of anti-correlation may vary according to the source region and the rupture mechanism of each earthquake. Meanwhile, the relations between the radiated energy-to-moment ratio, E_R/ M_o, and M_o from the models show positive correlations, but the case of SWM shows much higher correlation comparing to the case of EBM. The higher correlation is due to the relation between M_o and *k*, which also means that the law of self-similarity does not hold as shown by Abercrombie, and Kanamori and Rivera. Finally, the fault rupture areas estimated from two models also depict different relation to M_o, and the differences mainly come from the different relations between M_o and *k* in each model. The relation between fault rupture area and M_W from SWM is comparable to the recently obtained result by Allen and Hayes.

Keywords: Self-similarity; Scaling relation; Slip-weakening model; Rupture velocity; Source-controlled f_{max}

1. Introduction

Since Aki [1] found the law of self-similarity, the law has been tested by many researchers and the results have brought the pros and cons on its availability. Many researches, e.g. references in [2], show that the stress drop (and/or apparent stress) have a positive correlation to the size of earthquakes, and some researchers assert that the positive correlation may come from the missing data [3]. Whereas Baltay et al. [4] claim that such correlation can be weakened by using a stacked coda amplitude spectrum as an empirical Green's function and, eventually, the law is sustained because of the weak correlation. Almost all these results derived from the same static scaling relation from the static circular fault model by Eshelby [5] and Keylis-Borok [6] with Brune's nondimensional corner frequency [7]. On the other hand, Causse and Song [8] show that the variability of peak ground acceleration from GMPEs is reduced if we assume an anti-correlation between the stress drop and the rupture velocity. The reduction of variability may be interpreted as an evidence of the model improvement. Meanwhile, Tinti et al. [9] show the existence of such anti-correlation from the numerical rupture simulations using a regularized Yoffe function as a slip-rate function in kinematic modeling. The simulation results also show that the relations between scaling parameters are consistent with those from the slip-weakening model developed by Ohnaka and Yamashita [10]. On the other hand, Bizzari [11,12] compared various slip-weakening models including rate- and state-dependent model by incorporating them into the 3-D dynamic rupture simulations. The comparisons show an equivalency

between various slip-weakening models. It also shows a dependence of rupture velocity on the size of earthquakes which means that the law of self-similarity should be verified under the consideration of interdependencies between scaling parameters and rupture velocity as well as the relation between rupture velocity and the size of earthquakes. If the stress drop has an anti-correlation to the rupture velocity, the rupture velocity would have a positive correlation to the size of earthquakes to hold the law of self-similarity.

In this paper, two representative models for scaling relation, i.e. Eshelby and Keylis-Borok's model with Brune's nondimensional corner frequency (hereafter EBM), and Ohnaka-Yamashita's slip-weakening model (hereafter SWM), are compared. Since a direct comparison between both models is not possible due to the nature of SWM describing the scaling relation within a breakdown zone, the SWM is firstly extended beyond the breakdown zone and correlations between scaling parameters and the size of earthquakes from each model are investigated.

2. EBM and SWM extension

2.1 Basic assumptions

The fault is assumed as a circular fault for simplicity. The size of an earthquake is mainly expressed by the seismic moment ($M_o=\mu DA$ in Nm, in which μ is the shear modulus of a fault, D is the spatial average value of final slip displacement over the fault and A is a fault rupture area, which is defined by $A=\pi r^2$ using the fault radius r), but the moment magnitude M_W is also used according to the purpose and it is defined by the following equation.

$$M_W = \frac{2}{3}\log_{10} M_o - 6.03 \tag{1}$$

Since D and A can be different according to the used scale relationship for the same seismic moment, each parameter is distinguished by subscript, i.e. "*e*" for EBM and "s" for SWM. The spectral characteristics of slip displacement are assumed to follow ω^{-2} model, e.g. Brune's model [7]. The Fourier amplitude spectrum is characterized by the corner frequency f_c, which is assumed to be equivalent to the inverse of the total duration of source time function, e.g. [13]. On the other hand, the rise time τ is defined by $1/2\pi f_c (=1/\omega_c)$. Denoting the rupture velocity as V_r, the corner frequency can be expressed as follows.

$$f_c = \frac{1}{T_r} = \frac{V_r}{r} \tag{2}$$

The corner frequency can also be expressed as a nondimensional form by introducing a nondimensional number k, which is defined by the ratio of rupture velocity to the S wave velocity V_s. That is,

$$k = \frac{V_r}{V_S} \tag{3}$$

Then,

$$\frac{f_c r}{V_r} = \frac{f_c r}{k V_S} = 1 \tag{4}$$

In the derivation of Brune's model, k was assumed as $2.32/2\pi \simeq 0.372$. If we define a nondimensional corner frequency as $f_c r/V_s$, then k corresponds to the nondimensional corner frequency. Eq. (4) is the simplest mathematical expression for what we have to treat in this study and called the dynamic similarity, e.g. [13].

2.2 Eshelby-(Keylis-Borok)-Brune's model (EBM)

Let us consider a static shear fracture problem of a circular fault of radius r_e with the conditions where the slip is constrained inside the fault, i.e. $D(r)=0$ for $r \geq r_e$, and is a maximum at the center of the fault, $D(0)=D_{max}$. The stress far from the fault has a constant value and is zero inside the fault for $r<r_e$. Then, the

stress drop $\Delta\sigma_e$ is equal to the constant stress far from the fault. Under these conditions, the stress drop can be expressed by the following equation [5, 6].

$$\Delta\sigma_e = \frac{7}{16} M_o \left(\frac{f_c}{kV_s} \right)^3 \tag{5}$$

Substituting Brune's nondimensional corner frequency, i.e. $k = 0.372$, into the above equation, we can get the most widely used static scaling relationship. That is,

$$\Delta\sigma_e = 8.5 M_o \left(\frac{f_c}{V_s} \right)^3 \tag{6}$$

As shown in Eq. (6), EBM states that the stress drop is a constant as $M_o \propto f_c^{-3}$ or $f_c \propto M_o^{-1/3}$.

Kanamori and Rivera [2] investigated the static and dynamic scaling relations together based on the results from reliable previous studies and provided a modified relationship between M_o and f_c with a conclusion that the rupture velocity and the stress drop are key parameters for understanding the rupture physics. The modified relationship between M_o and f_c can be expressed by

$$f_c \propto M_o^{-1/(3+\varepsilon)} \tag{7}$$

Meanwhile, Oth et al. [14] investigated earthquake source characteristics and scaling properties using the results of a spectral inversion of more than 29,000 accelerometric borehole recordings from 1,826 earthquakes throughout Japan and reported the values of ε for two cases in which focal depth is less than 30 km (crustal events) and deeper than 30 km (subcrustal events). The statistical characteristic values of ε, i.e. mean $\pm$ standard deviation, are 0.12 ± 0.12 for the crustal events and 0.18 ± 0.08 for the subcrustal events, which are far smaller than the values of 0.5~1.0 reported by Mayeda et al. [15] for the western part of US and Yoo et al. [16] for the Korean peninsula. Baltay et al. [4] indicated that a possible reason for large differences in ε-estimates is the limited frequency bandwidth (or a poor dynamic range) in used records.

On the other hand, from Eq. (4), ε can be analyzed by the terms related to k and r. In which, since r can be substituted by the square root of a fault rupture area, the latter relationship can be changed by that between $A^{1/2}$ and M_o. Moreover, if the relationship between k and M_o is known, the relationship between $A^{1/2}$ and M_o is then straightforward. Therefore, we mainly shed light on the relationship between k and M_o.

2.3 Slip-weakening model (SWM)

There are various models to express the slip-weakening behavior in shear fracture. Among those models, as outlined in the introduction, the model developed by Ohnaka and Yamashita ([10], hereafter OY89) may be appropriate to investigate the effect of rupture velocity on the scaling relations comparing to EBM. OY89 provided a constitutive relationship to describe the slip-weakening behavior from the series of laboratory experiments for the shear failure of granite and derived a scaling relation from the theoretical and numerical analyses of the constitutive relationship. The derived scaling relation is as follows:

$$\sigma_p = c_\Gamma \mu \pi^2 C_a(k) \frac{D_c}{X_c} \tag{8}$$

in which, σ_p indicates the peak stress at the end of slip-strengthening from the initial stress σ_i and c_Γ is a constant to express the effect of the stress ratio of the initial stress to the peak stress and of the stress drop on the slip-weakening behavior. OY89 investigated the effect of the stress ratio (σ_i / σ_p=0.5~0.8) and suggested 0.53 as c_Γ (Eq. (38) in [10]). D_c is a critical slip displacement which corresponds to the slip displacement for when the shear stress drops to $0.15\sigma_p$ from the peak stress in slip-weakening process and X_c is the breakdown zone length measured from the rupture front. $C_a(k)$ is a k-dependent coefficient related to the stress-intensity factors in fracture mechanics [17], which is different for each mode of shear fracture denoted by subscript a. That is, if Poisson material is assumed,

$$C_{II}(k) = 2\left[\sqrt{1-k^2/3} - \left(1-k^2/2\right)^2 / \sqrt{1-k^2}\right] / \pi k^2 \tag{9a}$$

for in-plane fracture mode and for anti-plane fracture mode,

$$C_{III}(k) = \sqrt{1-k^2} / 2\pi \tag{9b}$$

Since the two modes of shear fracture are generally appeared simultaneously in a rupture process, $C_a(k)$ is assumed by the following equation for simplicity.

$$C_a(k) = \sqrt{\left[C_{II}^2(k) + C_{III}^2(k)\right] / 2} \tag{10}$$

It is noteworthy that the peak stress σ_p in Eq. (8) has changed to the breakdown stress drop $\Delta\sigma_b$ after OY89 (e.g. references in [18]). In this study, we call the peak stress the stress drop in SWM and denote as $\Delta\sigma_s$. Actually, $\Delta\sigma_b$ indicates the stress difference between the peak stress and the (dynamic) friction stress, which was neglected in OY89 as is usual practice. And, in general, $\Delta\sigma_b$ is assumed to be proportional to the peak stress and the proportionality is reflected in c_Γ. Moreover, since it is obvious that the definitions of stress drop in EBM and SWM are quite different, the quantitative comparison of the stress drops should be made from the viewpoint of σ_i / σ_p under the same k. For example, assuming k =0.372 gives σ_i / σ_p=0.64 from the following extended SWM.

2.4 SWM extension

As aforementioned, Eq. (8) describes the scaling relation within a breakdown (or cohesive) zone. In order to compare the property of Eq. (8) to EBM, the scaling relation should be extended to the whole fault area. For such purpose, let us assume that the extended scaling relation can be expressed by the following equation.

$$\Delta\sigma_s = \mu C_s \frac{D_s}{r_s} \tag{11}$$

Since the stress drop $\Delta\sigma_s$ is a fault rupture driving force, it can be considered as a unique quantity for a specified event. Therefore, we can equate the righthand sides of Eq. (8) and Eq. (11). Then, the coefficient C_s can be written by the following equation.

$$C_s = c_\Gamma \pi^2 C_a(k) \frac{D_c / X_c}{D_s / r_s} \tag{12}$$

In which, D_c / D_s and r_s / X_c are closely related to the dynamic characteristics of rupture process. Firstly, D_c / D_s is closely related to the seismic energy radiation efficiency η_R, which is defined by the ratio of radiated energy E_R to potential energy ΔU, i.e. $\eta_R = E_R / \Delta U$. The potential energy is generally expressed by the sum of fracture energy E_G and radiated energy E_R, i.e. $\Delta U = E_G + E_R$. Therefore, the radiation efficiency η_R can be written by the following equation.

$$\eta_R = 1 - \frac{E_G}{\Delta U} \tag{13}$$

On the other hand, ΔU and E_G can be approximated by $E_G = 1/2 \Delta\sigma_s D_c A_s$ and $\Delta U = 1/2 \Delta\sigma_s D_s A_s$, respectively. Consequently, the radiation efficiency η_R can be expressed by using D_c / D_s, i.e. $\eta_R = 1 - D_c / D_s$. Therefore,

$$\frac{D_c}{D_s} = 1 - \eta_R \tag{14}$$

Secondly, the ratio r_s / X_c can be rewritten as follows by the assumption for the source-controlled cutoff frequency in a specific barrier model by Papageorgiou and Aki [19].

$$\frac{r_s}{X_c} = \frac{r_s / V_r}{X_c / V_r} = \frac{f_{\max}^s}{f_c} \tag{15}$$

In which, $f_{\max}^s$ is a source-controlled cutoff frequency in a high frequency range of amplitude spectrum. OY89 independently defined $f_{\max}^s$ as an inverse of the time taken by the stress drop from the peak stress. The time is equivalent to the slip-weakening duration, T_c, i.e. $T_c = X_c / V_r$ [18]. Consequently, the coefficient C_s can be written by the following equation.

$$C_s = c_\Gamma \pi^2 C_a(k)(1-\eta_R)\frac{f_{\max}^s}{f_c} \tag{16}$$

3. *k*-dependence of the scaling relations

3.1 *k*-dependence of radiation efficiency

Radiation efficiency η_R can be estimated independently from rupture velocity V_r, e.g. [20]. The ratio of rupture velocity and limiting rupture speed can be related to the radiation efficiency by

$$\eta_R = 1 - g_a(V_r) \tag{17}$$

in which $g_a(V_r)$ is a unique function of rupture velocity. For in-plane mode shear crack,

$$g_{II}(V_r) = (1 - V_r / V_R) / \sqrt{1 - V_r / V_s} \tag{18a}$$

and for anti-plane mode shear crack,

$$g_{III}(V_r) = \sqrt{(1 - V_r / V_s)/(1 + V_r / V_s)} \tag{18b}$$

In which, V_R is the Rayleigh wave velocity as a limiting rupture velocity and can be expressed by the ratio to V_s, i.e. $V_R \simeq 0.92 V_s$ for Poisson material.

For sub-shear velocity rupture, i.e. $V_r < V_R$, the differences between $g_{II}(V_r)$ and $g_{III}(V_r)$ are not so significant. And, from the same reasoning for $C_a(k)$, $g_a(V_r)$ may be approximated by the following function of *k*.

$$g_a(k) = \sqrt{\left[g_{II}^2(k) + g_{III}^2(k)\right]/2} \tag{19}$$

3.2 *k*-dependence of $f_{\max}^s / f_c$

Before investigating the *k*-dependence of $f_{\max}^s / f_c$, it is necessary to define the seismic energy radiation in frequency domain. The total energy radiated by the point source across a spherical surface surrounding the source can be written in frequency domain by the following equation, e.g. [13];

$$E_R = E_p + E_s = \frac{1}{4\pi^2 \rho}\left(\frac{\langle R_p^2 \rangle}{V_p^5} + \frac{\langle R_s^2 \rangle}{V_s^5}\right)\int_0^\infty \omega^2 \left|\dot{M}_o(\omega)\right|^2 d\omega \tag{20}$$

in which, ρ is the density of material around the fault, $\langle R_p^2 \rangle$ and $\langle R_s^2 \rangle$ are mean values of the squared radiation pattern coefficients for P and S waves over the surface of the focal sphere, respectively. Considering that $E_s \gg E_p$ [21, 22], the total radiation energy can be approximated by E_s only. Assuming a generic ω^{-2} model for source time function, i.e. $\dot{M}_o(\omega) = M_o / \left[1 + (\omega / \omega_c)^2\right]$, 2/5 for $\langle R_s^2 \rangle$ [23], and applying $V_s^2 = \mu / \rho$, Eq. (20) can be written approximately as follows.

$$E_R \simeq E_s = \frac{\langle R_s^2 \rangle}{4\pi^2 \rho V_s^5} \int_0^\infty \omega^2 \left| \dot{M}_o(\omega) \right|^2 d\omega = \frac{\pi^2}{5\mu} M_o^2 \left(\frac{f_c}{V_s} \right)^3 \tag{21}$$

Furthermore, substituting the definitions of M_o and ΔU, and Eqs. (2), (3) and (11) into the above equation, the radiation efficiency can be approximated by

$$\eta_R^\infty = \frac{E_R}{\Delta U} \simeq \frac{2\pi^3}{5} \frac{\mu}{\Delta\sigma_s} \frac{D_s}{r_s} k^3 \simeq \frac{12.4k^3}{C_s} \tag{22}$$

in which, the symbol ∞ indicates the case satisfying the condition of $f_{\max}^s \to \infty$. As such, $f_{\max}^s / f_c$ can be expressed by the following equation from Eqs. (16) and (22).

$$\frac{f_{\max}^s}{f_c} \simeq \frac{12.4k^3}{c_\Gamma \pi^2 C_a(k)\left(1-\eta_R^\infty\right)\eta_R^\infty} \tag{23}$$

However, the condition of $f_{\max}^s \to \infty$ may never be satisfied by the definition of $f_{\max}^s$. In order to satisfy the condition, X_c must shrink to zero for a finite rupture velocity and this means zero slip-weakening distance in rupture process. Consequently, it may be said that the limited frequency bandwidth is an inherent nature of rupture process in so far as we see the process as a slip-weakening behavior. For $f_{\max}^s \ll \infty$, the integral in Eq. (21) should be corrected considering the limited frequency bandwidth by the following approximation [24].

$$\int_0^{2\pi f_{\max}^s} \omega^2 \left| \dot{M}_o(\omega) \right|^2 d\omega \simeq c_f \int_0^\infty \omega^2 \left| \dot{M}_o(\omega) \right|^2 d\omega \tag{24}$$

In which,

$$c_f = \frac{2}{\pi}\left(\tan^{-1} k_f - \frac{k_f}{1+k_f^2} \right), \quad k_f = \frac{f_{\max}^s}{f_c} \tag{25}$$

Then, Eq. (23) becomes

$$\frac{f_{\max}^s}{f_c} \simeq \frac{12.4k^3}{c_\Gamma \pi^2 C_a(k)\left(1-c_f\eta_R^\infty\right)\eta_R^\infty} \tag{26}$$

By the way, if we assume that Eqs. (17)~(19) correspond to η_R^∞, $f_{\max}^s / f_c$ depends only on *k*. Therefore, if it is possible to find $f_{\max}^s$ as well as f_c from a measured record, *k* can be inferred from Eq. (26) and related equations. Using inferred *k*, $A_s(=\pi r_s^2)$ and D_s can be estimated from f_c and M_o, respectively. Eventually, the stress drop $\Delta\sigma_s$ is also determined from Eq. (11), in which C_s can be approximated by $14.6k^{1.94}$ and becomes unity for $k \simeq 0.25$. As such, $c_f\eta_R^\infty \simeq 0.05$ which may correspond to a minimum radiation efficiency.

4. Application example

Source-controlled cutoff frequency has been rarely treated comparing to other source parameters since it is quite difficult to distinguish its existence from usual spectral inversion analysis. The debate on whether the cutoff frequency in acceleration spectrum is a source-controlled parameter or a site-controlled parameter still goes on. On the other hand, Kinoshita [25] carefully investigated $f_{\max}^s$ of bedrock motion in the Tokyo metropolitan area and obtained a result that $f_{\max}^s$ depends on source region. For example, $f_{\max}^s$ is less than 10Hz for the source region located at the collision area between the Philippine Sea plate, the Pacific and the Eurasian plates, whereas the values higher than 20Hz are obtained for other inter-plate zone between the Pacific and the Eurasian plates. Meanwhile, Satoh et al. [26] investigated 18 offshore earthquakes in Kanto and Tohoku regions (focal depth 0~73km, M_{JMA} 3.4~7.1, epicenters 35.7~39.85N, 140.72~143.75E), and

reported $f_{\max}^{s}$ of 9.92~22.91Hz with f_c values (see Table 3 in [26]). The obtained values of $f_{\max}^{s}$ are distributed between two boundary values obtained by Kinoshita. Furthermore, Satoh et al. [27] examined the relation between $f_{\max}^{s}$ and M_o, and the relation between $f_{\max}^{s}$ and $\Delta\sigma_e$ in order to quantitatively evaluate spectral amplitudes in high frequency range based on the acceleration records of 50 offshore earthquakes records (focal depth 35~93km, M_{JMA} 4.0~6.6, epicenters 36.2~37.9N, 140.5~142.0E) from the boreholes at GL-330m in Iwaki and GL-950m in Tomioka, Japan. The obtained $f_{\max}^{s}$ (7.3~25.1Hz) are similar to the values shown in [26] and also found the source region dependence of $f_{\max}^{s}$ (see Table 1 in [27]).

In order to examine the availability of extended SWM, we selected 43 events among 68 events listed in [26] and [27]. In that selection, the data from the events occurred at the focal depth shallower than 30km are excluded from reference [26] and the data from zones A~C in reference [27] are added considering that the fault environment at deeper focal depth is rather homogeneous than the shallower ones. Additionally, 15 f_c-data compiled by Baltay et al. [28] from Hi-net records of the repeated earthquake sequence offshore of Kamaishi, Iwate (focal depth 46.1~65.1km, M_W2.1~4.64, epicenters 39.34~39.37N, 142.06~142.10E) in the period of 2003~2008 are also used, though $f_{\max}^{s}$ are unknown. The data draw important implications in application.

The used f_c-data are shown in Fig.1 with a regression line. In the figure, open circles indicate the data from Kamaishi [28] and solid circles are for the data from [26, 27]. The regression line shows that M_o-f_c relation fairly well coincides with that by Oth et al. for subcrustal events [14]. From the slope of regression line (-0.319), ε in Eq. (7) is estimated as 0.13, which is slightly smaller than the mean value (0.18) but within the range of mean $\pm$ standard deviation (0.08).

Derived M_o-k_f relation is shown in Fig.2 with a regression line. The figure clearly shows a positive correlation between M_o and k_f, and the regression line indicates that the relation is mainly due to M_o-f_c relation. From comparing the slopes, it is easily found that $f_{\max}^{s} \propto M_o^{0.04}$.

In Fig. 3, M_o-k relation from Eq. (26) is shown with a regression line and a reference relation from the fully 3-D dynamic spontaneous rupture simulations using slip-weakening models by Bizzarri [12]. The original result obtained by Bizzarri was not for the M_o-k relation but for the relations of the spatial mean peak slip velocity over the fault rupture area, say V_{peak}, to k and M_o. Those are $V_{peak} = 0.67\exp(2.89k)$ and $V_{peak} = bM_o^{0.18}$, respectively. In which, b is an appropriately chosen constant. Equating two equations with respect to V_{peak}, the M_o-k relation is obtained. That is, assuming b as 1/330, which corresponds to the lower bound of the simulation results, two equations result in k=0.062lnM_o-1.868, and the result is quite similar to the regression line for the used data in this study, i.e. k=0.054lnM_o-1.526, as shown in the figure. It is remarkable that the correlated M_o-k relation contradicts to the usual assumption. For example, Abercrombie and Rice [29] supposed a constant rupture velocity in the study on the relation between earthquake scaling and slip-weakening. They also indicated that if the slip expanded at a smaller rupture velocity, it would then reach a smaller source dimension in the duration of the recorded pulse, and the stress drop over the slip area would be much higher, and raised a question about how the faults can sustain such stresses. They concluded that the assumption of a constant rupture velocity seems the most appropriate until convincing evidence suggests otherwise.

By the way, the type of regression function is problematic related to the limitation on k_f. That is, k_f should be greater than unity since $X_c < r_s$ in Eq. (15). In order to satisfy the limitation, k should be greater than about 0.24 from Eq. (26). On the other hand, if we try to apply the derived M_o-k relation to smaller size earthquakes, e.g. $M_o < 10^{15}$ Nm like the case of Kamaishi, the limitation is violated by the derived relation. This also means that the nearly independent $f_{\max}^{s}$ on M_o is problematic to hold the physical limitations on k_f as well as k. From such reasons, the estimates of $f_{\max}^{s}$ for relatively small size of earthquakes shown in [26, 27] seem erroneous and k should decrease asymptotically to its limiting value with M_o. To avoid any severe violation, power function may be more appropriate to express M_o-k relation, even though the residuals from

the regression line increase and the violation still remains unfixed. In the following discussion, Eq. (27) is assumed as M_o-k relation for the case of Kamaishi and shown in Fig.3 for comparison.

$$k = 0.011 M_o^{0.1} \tag{27}$$

The establishment of the law of self-similarity depends on whether the stress drop and/or the apparent stress depend(s) on the size of earthquakes. The M_o-$\Delta\sigma$ relations from EBM and SWM are shown in Fig.4. Based on the regression lines, EBM shows a weak positive correlation between M_o and $\Delta\sigma_e$, whereas SWM gives a weakly anti-correlated relation between two quantities. But the absolute values of the slopes of M_o-$\Delta\sigma$ relations are almost the same. Such anti-correlation is also indicated by Kanamori and Rivera [2] which implies that small earthquakes represent failures of small-scale asperities with high stress concentration. It is also noteworthy that those correlation characteristics are strongly affected by the data from Kamaishi, but the stress drops are not so excessively large as Abercrombie and Rice [29] questioned. Excluding the data from Kamaishi, both models show similar tendencies and the law of self-similarity seems to be available, even though there are extraordinarily large stress drops in the range of $M_0 = 10^{15\sim16}$ Nm. Those values are due to larger f_c and lower k_f, which lead to lower values of k.

When SWM is applied to the data, k-$\Delta\sigma_s$ relation is easily obtained. The obtained result is shown in Fig.5. From the figure, it may be possible to make two analogies. One is the existence of strong anti-correlation between k and $\Delta\sigma_s$ as expected by Causse and Song [8], if we exclude the data from Kamaishi because of the lack of information on $f_{\max}^s$. The other analogy is that fairly weak anti-correlation or nearly independent relation between two quantities may exist if we ignore the cases shown higher stress drops than 100MPa as extraordinary cases. Meanwhile, Tinti et al. [9] indicated strong anti-correlation between k and $\Delta\sigma_s$ through the 3-D dynamic rupture simulations, and a general hypothesis that larger-scale earthquakes show smaller stress drops because the larger-scale earthquakes usually occur on mature faults also supports the anti-correlation. If the hypothesis is true, the relation between k and $\Delta\sigma_s$ for Kamaishi is skeptical from the fact that Kamaishi has experienced repeating earthquake sequences and the main earthquake recurs every 5~6 years with M_W 4.9 ± 0.2 since 1957. Between repeats, many smaller earthquakes, which are used in this study, rupture similar patches on the deepest part of the inter-plate main thrust zone, at about 50km depth [28, 30]. Such fault conditions may reflect a mature fault and greater k would be appropriate for the case of Kamaishi, which is also supported by the relatively enriched high frequencies in the main events [28].

On the other hand, Venkataraman and Kanamori [20] computed the radiated energy for 23 subduction zone earthquakes recorded between 1992 to 2001 and suggested that differences in the radiation efficiencies of different types of earthquakes could be due to fundamental differences in their rupture mechanics. It is obvious that the radiation efficiency depends on k as shown in Eqs. (17)~(22). Therefore, k also can vary according to the rupture mechanics in each earthquake. Moreover, Kanamori and Rivera [2] also indicated that small and large earthquakes can have significantly different static stress drops and rupture velocities; if the ratio $\tilde{e}$, which is defined by the ratio E_R/M_o, varies with the size of an earthquake, the difference can even be larger. Meanwhile, it is difficult to estimate E_R accurately because of the complex wave propagation effect and, for small earthquakes, the limited frequency bandwidth of the record. The relations between M_o and $\tilde{e}$ for the used data are shown in Fig.6. The relations from EBM and SWM both show a positive correlation between M_o and $\tilde{e}$, but the relation from SWM gives much higher correlation, which is mainly due to Eq. (27). Additionally, it is also remarkable that the relation from SWM is comparable to that from the previous studies compiled by Kanamori and Rivera (see Figure.1 in [2]). Especially, the values of $\tilde{e}$ from Abercrombie [21] are quite similar to those from SWM for Kamaishi. Such similarity comes from the assumed small k. Abercrombie estimated $\tilde{e}$ by integrating the velocity squared spectra of the records over the limited frequency ranges in which the upper bound of frequency ranges was set to be greater than $5f_c$. Oth et al. [14] asserted that such relatively small $\tilde{e}$ is due to the limited frequency bandwidth. However, the assertion is questionable because the high frequency spectral falloff rates may be underestimated due to the disregarding the frequency dependence of Q-factor, e.g. [31], and the underestimated falloff rates may compensate the effect of the limited frequency bandwidth in the integration. Moreover, the listed spectral falloff rates in [21] increase with f_c. This indicates that the smaller $\tilde{e}$ comes from the f_c-dependent falloff rate.

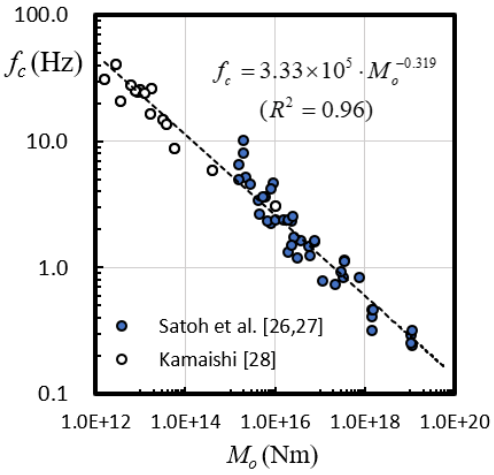

Fig. 1 – Relation between M_o and f_c

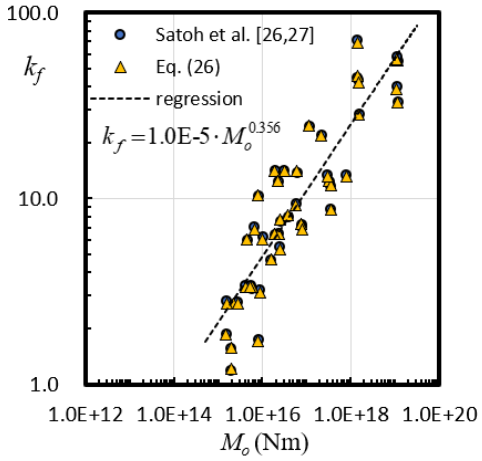

Fig. 2 – Relation between M_o and k_f, $k_f = f^s_{\max} / f_c$

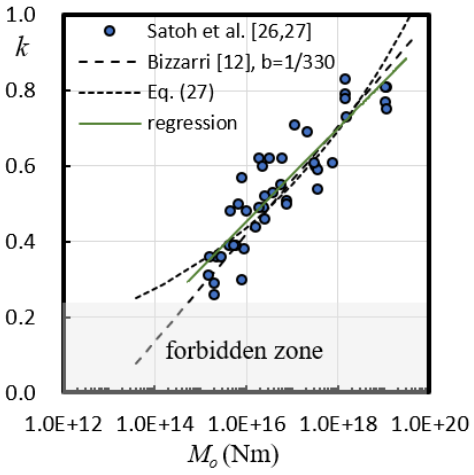

Fig. 3 – Relation between M_o and k, $k = V_r / V_s$

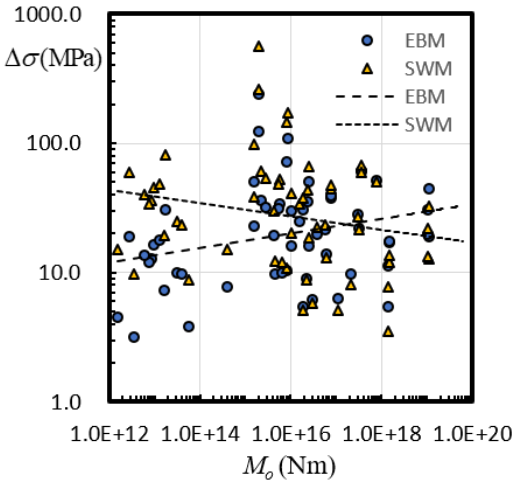

Fig. 4 – Relation between M_o and stress drop $\Delta\sigma$

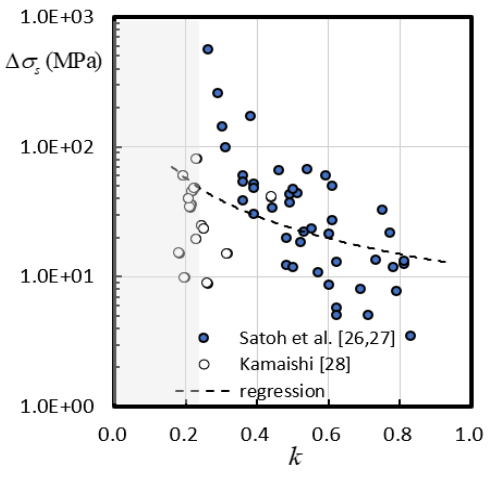

Fig. 5 – Relation between k and $\Delta\sigma_s$

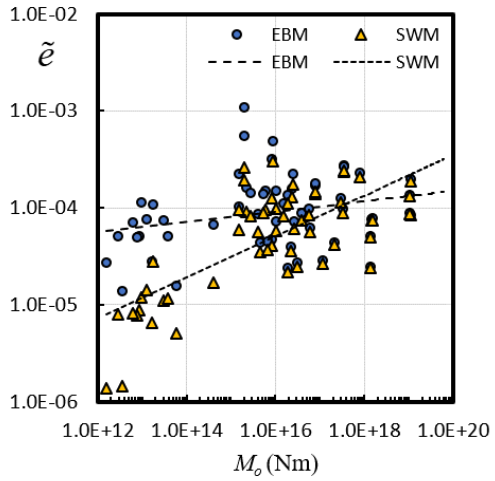

Fig. 6 – Relation between M_o and $\tilde{e}$, $\tilde{e} = E_R / M_o$

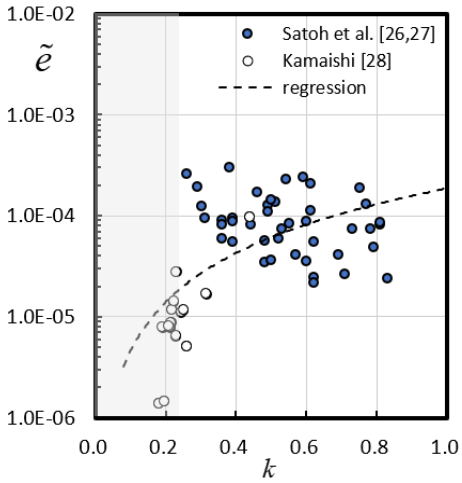

Fig. 7 – Relation between k and $\tilde{e}$, $\tilde{e} = E_R / M_o$

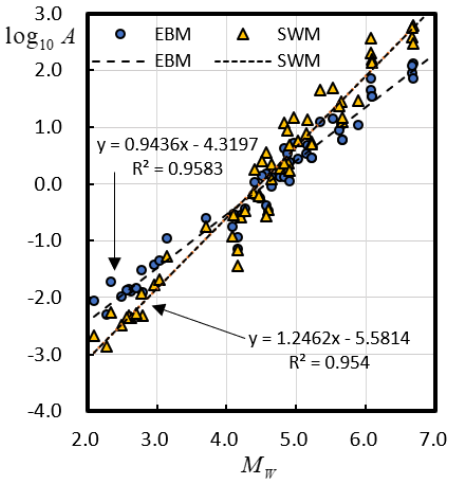

Fig. 8 – Relation between M_W and $\log_{10} A\,(\mathrm{km}^2)$

The relation between k and $\tilde{e}$ is shown in Fig.7. As shown in the figure, the values of $\tilde{e}$ for Kamaishi are about 10 times smaller than those from the data compiled by Satoh et al., whereas the value of $\tilde{e}$ from the main shock ($M_o \simeq 10^{16}$ Nm, $k \simeq 0.44$) is quite similar to those from other relatively larger events. Those smaller $\tilde{e}$ come from c_f in Eqs. (24)~(25), i.e. the limited frequency bandwidth due to the assumed small k. Excluding the results for M_o <10^{15} Nm or assuming larger k for smaller earthquakes, $\tilde{e}$ seems to be independent on k and the independence of $\tilde{e}$ on M_o might also be available. However, such assumption may not make sense because it is obvious that M_o-dependent k and k_f result in the increase of high frequency spectral falloff rates as M_o decreases, even though Eq. (27) is a faulty assumption considering the limitations on k and k_f shown as the shaded zone in the figures. Moreover, if we assume a generic ω^{-2} model for the case of a sufficiently large k_f or M_o, and that the effect of the source-controlled cutoff frequency in a high frequency range can be modeled by two-pole Butterworth low-pass filter like the model by Satoh et al. [26, 27], the high frequency spectral falloff rate then increases from 2.0 to 4.0 when k_f decreases to unity with M_o. Meanwhile, if we assume the frequency dependence of Q-factor as $Q(f) = Q_o \cdot f^{0.6\sim0.7}$ (e.g. Fig.3 in [31]), the spectral falloff rates shown in [21] vary with M_o in a similar way. Consequently, it can be said that the small $\tilde{e}$ and large ε eventually come from the source-controlled cutoff frequency.

Kanamori and Anderson [32] found the linear relationship with a slope of 2/3 between $\log_{10}A$ and $\log_{10}M_o$. This linear relationship is usually expressed by the following linear equation.

$$\log_{10} A = c_1 M_W - c_2 \tag{28}$$

For a circular fault, the theory gives 1.0 for c_1 and about 4.0 for c_2 when the constant stress drop of 3MPa is assumed. Many researches have tried to estimate c_1 and c_2 according to the type of fault and source region, and obtained similar values to the theoretical values. The relations from EBM and SWM are shown in Fig.8. In the estimation of A (km^2), Eq. (4) and V_s values in the references are used. As shown in the figure, two models give very different results for relatively large earthquakes. For the case of SWM, the obtained c_1 (1.25) and c_2 (5.58) are quite similar to those obtained by Allen and Hayes [33] for M_W 7.1~8.63 subduction interface earthquakes, i.e. c_1=1.22 and c_2=5.62, using a database of consistently derived finite-fault rupture models from teleseismic inversion. On the other hand, EBM gives 0.94 and 4.32 for c_1 and c_2, respectively. The c_2 larger than 4.3 are generally reported for stable continental regions under the constraint of c_1=1.0 [34].

5. Conclusion

The scaling relation based on slip-weakening model originally developed by Ohnaka and Yamashita is extended beyond the breakdown (or cohesive) zone and the source properties from the extended model

(SWM) are compared to those from the most widely used model by Eshelby and Keylis-Borok with Brune's nondimensional corner frequency (EBM). SWM shows that the source properties greatly depend on the rupture velocity ratio to S wave velocity, say k, which is determined from the spectral corner frequency and the source-controlled cutoff frequency. From the comparison, two models show different correlation characteristics between the scaling parameters and the size of earthquakes. For the case of stress drop, two models show contradict correlation characteristics to the size of earthquakes, but the correlation from each model is relatively weak. On the other hand, SWM gives anti-correlation between stress drop and rupture velocity (ratio) as expected by Causse and Song. The degree of anti-correlation may vary according to the source region and the rupture mechanism of each earthquake. Meanwhile, the relations between E_R/M_o and M_o from the models show positive correlations, but the case of SWM shows much higher correlation comparing to the case of EBM. Such higher correlation is comparable to the results from the previous studies compiled by Abercrombie, and Kanamori and Rivera. Especially, the dependence of E_R/M_o on M_o obtained by Abercrombie can be explained by the dependence of high frequency spectral falloff rate on the size of earthquakes, which coincides to the derived relationships in this study. Therefore, it can be concluded that the scaling relation between source parameters from SWM depends on a source region and the scaling parameters, especially the dynamic scaling parameter $\tilde{e}$, depend on the size of earthquakes. It means that the law of self-similarity does not hold. Finally, the fault rupture areas estimated from the two models also depict different relations to the size of earthquakes, and the differences come from the different M_o-k relations used in each model. Comparing to the previous studies, SWM gives a more comparable result than EBM.

Acknowledgements

This research was supported by a grant (19RERP-B099826-05) from Residential Environment Research Program (RERP) funded by the Ministry of Land, Infrastructure and Transport of Korean government.

References

[1] Aki K (1967): Scaling law of seismic spectrum. *J. Geophys. Res.*, **73**, 5359-5376

[2] Kanamori H, Rivera L (2004): Static and dynamic scaling relations for earthquakes and their implications for rupture speed and stress drop. *Bull. Seism. Soc. Am.*, **94** (1), 314-319

[3] Ide S, Beroza GC (2001): Does apparent stress vary with earthquake size? *Geophys. Res. Lett.*, **28** (17), 3349-3352

[4] Baltay A, Ide S, Prieto G, Beroza GC (2010): Radiated seismic energy from coda measurements and no scaling in apparent stress with seismic moment, *J. Geophys. Res.*, **115**, B08314, doi:10.1029/2009JB006736

[5] Eshelby JD (1957): The determination of the elastic field of an ellipsoidal inclusion, and rotated problems. *Proc. Roy. Soc. Ser. A*, **241** (1226), 376-396, doi:10.1098/rspa.1957.0133

[6] Keylis-Borok BV (1959): Methods and results of the investigation of earthquake source and of source dimensions. *Ann. Geofisica*, **12**, 205-214

[7] Brune JN (1970): Tectonic stress and the spectra of seismic shear waves from earthquakes. *J. Geophys. Res.*, **75** (26), 4997-5009, doi:10.1029/JB091iB02p02095

[8] Causse M, Song SG (2015): Are stress drop and rupture velocity of earthquakes independent? Insight from observed ground motion variability. *Geophys. Res. Lett.*, **42**, 7383-7389, doi:10.1002/2015GL064793

[9] Tinti E, Fukuyama E, Piatanesi A, Cocco M (2005): A kinematic source-time function compatible with earthquake dynamics. *Bull. Seism. Soc. Am.*, **95** (4), 1211-1223

[10] Ohnaka M, Yamashita T (1989): A cohesive zone model for dynamic shear faulting based on experimentally inferred constitutive relation and strong motion parameters. *J. Geophys. Res.*, **94** (B4), 4089-4104

[11] Bizzari A (2011): On the deterministic description of earthquakes. *Rev. Geophys.*, **49**, RG3002/2011, Paper No. 2011RG000356

[12] Bizzari A (2012): Rupture speed and slip velocity: What we can learn from simulated earthquakes? *Earth and Planetary Sci. Lett.*, **317-318**, 196-203, doi:10.1016/j.epsl.2011.11.023

[13] Udias A, Madariaga R, Buforn E (2014): *Source mechanisms of earthquakes, theory and practice*. Cambridge Univ. Press

[14] Oth A, Bindi D, Parolai S, Di Giacomo D (2010): Earthquake scaling characteristics and the scale-(in)dependence of seismic energy-to-moment ratio: Insight from Kik-net data in Japan. *Geophys. Res. Lett.*, **37**, L19304, doi:10.1029/2010GL044572

[15] Mayeda K, Walter WR (1996): Moment, energy, stress drop, and source spectra of western United States earthquakes from regional coda envelopes. *J. Geophys. Res.*, **101**, 11,195-11,208

[16] Yoo SH, Rhie JK, Choi HS, Mayeda K (2011): Coda-derived source parameters of earthquakes and their scaling relationships in the Korean peninsula. *Bull. Seism. Soc. Am.*, **101** (5), 2388-2398, doi:10.1785/0120100318

[17] Aki K, Richards PG (2002): *Quantitative seismology*. University Science Books, 2nd edition

[18] Ohnaka M (2013): *The physics of rock failure and earthquakes*. Cambridge Univ. Press

[19] Papageorgiou AS, Aki K (1983): A specific barrier model for the quantitative description of inhomogeneous faulting and the prediction of strong ground motion. I. Description of the model. *Bull. Seism. Soc. Am.*, **73** (3), 693-722

[20] Venkataraman A, Kanamori H (2004): Observational constraints on the fracture energy of subduction zone earthquakes. *J. Geophys. Res.*, **109**, B05302, doi:10.1029/2003JB002549

[21] Abercrombie RE (1995): Earthquake source scaling relationship from -1 to 5 M_L using seismograms recorded at 2.5-km depth. *J. Geophys. Res.*, **100** (B12), 24,015-24,036

[22] Kaneko Y, Shearer PM (2014): Seismic source spectra and estimated stress drop derived from cohesive-zone models of circular subshear rupture. *Geophys. J. Int.*, **197**, 1002-1015, doi:10.1093/gji/ggu030

[23] Boore DM, Boatwright J (1984): Average body-wave radiation coefficients. *Bull. Seism. Soc. Am.*, **74** (5), 1615-1621

[24] Lancieri M, Madariaga R, Bonilla F (2012): Spectral scaling of the aftershocks of the Tocopilla 2007 earthquake in northern Chile. *Geophys. J. Int.*, **188**, 469-480

[25] Kinoshita S (1992): Local characteristics of the f_{max} of bedrock motion in the Tokyo metropolitan area, Japan. *J. Phys. Earth*, **40**, 487-515

[26] Satoh T, Kawase H, Sato T (1997): Statistical spectral model of earthquakes in the eastern Tohoku district, Japan based on the surface and borehole records observed in Sendai. *Bull. Seism. Soc. Am.*, **87** (2), 446-462

[27] Satoh T, Kobayashi Y, Kawano H (2000): Stress drop and f_{max} estimated from strong motion records observed at deep boreholes in Japan. *Proc. 12th World Conference on Earthquake Engineering 12WCEE*, Paper No. 0251

[28] Baltay A, Ide S, Prieto G, Beroza G (2011): Variability in earthquake stress drop and apparent stress. *Geophys. Res. Lett.*, **38**, L06303, doi:10,1029/2011GL046698

[29] Abercrombie RE, Rice JR (2005): Can observation of earthquake scaling constrain slip weakening? *Geophys. J. Int.*, **162**, 406-424, doi:10.1111/j.1365-246X.2005.02579.x

[30] Uchida N, Matsuzawa T, Ellsworth W, Imanishi K, Shimamura K, Hasegawa A (2012): Source parameters of microearthquakes on an interplate asperity off Kamaishi, NE Japan over two earthquake cycles, *Geophys. J. Int.*, **189**, 999-1014, doi:10.1111/j.1365-246X.2012.05377.x

[31] Abercrombie RE (1998): A summary of attenuation measurements from borehole recordings of earthquakes: The 10Hz transition problem. *Pure appl. geophys*., **153**, 475-487

[32] Kanamori H, Anderson DL (1975): Theoretical basis of some empirical relations in seismology. *Bull. Seism. Soc. Am.*, **65** (5), 1073-1095

[33] Allen TI, Hayes GP (2017): Alternative rupture-scaling relationships for subduction interface and other offshore environments. *Bull. Seism. Soc. Am.*, **107** (3), 1240-1253, doi:10.1785/0120160255

[34] Somerville P (2014): Scaling relations between seismic moment and rupture area of earthquakes in stable continental regions. *PEER 2014/14*, Pacific Earthquake Engineering Research Center

